Unprivileged groups are less served by green cooling services in major European urban areas

Article

Accepted Version

Rocha, A. D. ORCID: https://orcid.org/0000-0001-6370-1240, Vulova, S. ORCID: https://orcid.org/0000-0001-9083-1163, Förster, M. ORCID: https://orcid.org/0000-0001-6689-5714, Gioli, B. ORCID: https://orcid.org/0000-0001-7631-2623, Matthews, B. ORCID: https://orcid.org/0000-0001-9710-7688, Helfter, C. ORCID: https://orcid.org/0000-0001-5773-4652, Meier, F. ORCID: https://orcid.org/0000-0003-0399-2757, Steeneveld, G.-J. ORCID: https://orcid.org/0000-0002-5922-8179, Barlow, J. F., Järvi, L. ORCID: https://orcid.org/0000-0002-5224-3448, Chrysoulakis, N. ORCID: https://orcid.org/0000-0002-5208-626X, Nicolini, G. ORCID: https://orcid.org/0000-0002-9800-3351 and Kleinschmit, B. (2024) Unprivileged groups are less served by green cooling services in major European urban areas. Nature Cities, 1 (6). pp. 424-435. ISSN 2731-9997 doi: 10.1038/s44284-024-00077-x Available at https://centaur.reading.ac.uk/123915/

Unprivileged groups are less served by green cooling services in major European urban areas

Article

Accepted Version

Rocha, A. D. ORCID: https://orcid.org/0000-0001-6370-1240, Vulova, S. ORCID: https://orcid.org/0000-0001-9083-1163, Förster, M. ORCID: https://orcid.org/0000-0001-6689-5714, Gioli, B. ORCID: https://orcid.org/0000-0001-7631-2623, Matthews, B. ORCID: https://orcid.org/0000-0001-9710-7688, Helfter, C. ORCID: https://orcid.org/0000-0001-5773-4652, Meier, F. ORCID: https://orcid.org/0000-0003-0399-2757, Steeneveld, G.-J. ORCID: https://orcid.org/0000-0002-5922-8179, Barlow, J. F., Järvi, L. ORCID: https://orcid.org/0000-0002-5224-3448, Chrysoulakis, N. ORCID: https://orcid.org/0000-0002-5208-626X, Nicolini, G. ORCID: https://orcid.org/0000-0002-9800-3351 and Kleinschmit, B. (2024) Unprivileged groups are less served by green cooling services in major European urban areas. Nature Cities, 1 (6). pp. 424-435. ISSN 2731-9997 doi: 10.1038/s44284-024-00077-x Available at https://centaur.reading.ac.uk/123915/

UNPRIVILEGED GROUPS ARE LESS SERVED BY GREEN COOLING SERVICES IN MAJOR EUROPEAN URBAN AREAS

Alby Duarte Rocha[1*], Stenka Vulova[1,2], Michael Förster[1], Beniamino Gioli[3], Bradley Matthews[4,5], Carole Helfter[6], Fred Meier[7], Gert-Jan Steeneveld[8], Janet F. Barlow[9], Leena Järvi[10], Nektarios Chrysoulakis[11], Giacomo Nicolini[12], Birgit Kleinschmit[1]

Heat stress is the leading climate-related cause of premature deaths in Europe. Major heatwaves have struck Europe recently and are expected to increase in magnitude and length. Large cities are particularly threatened due to the urban morphology and imperviousness. Green spaces mitigate heat, providing cooling services through shade provision and evapotranspiration. However, the distribution of green cooling and the population most affected are often unknown. We revealed environmental injustice regarding green cooling in fourteen major European urban areas. Vulnerable residents in Europe are not concentrated in the suburbs but in run-down central areas that coincide with low-cooling regions. In all studied areas, lower-income residents, tenants, immigrants and unemployed citizens receive below-average green cooling, while upper-income residents, nationals, and homeowners experience above-average cooling provision. The fatality risk during extreme heatwaves may increase as vulnerable residents are unable to afford passive or active cooling mitigation.

[1] Geoinformation in Environmental Planning Lab, Technische Universität Berlin, Germany. [2] Department of Environmental Meteorology, University of Kassel, Germany. [3] Institute of BioEconomy, National Research Council (IBE-CNR), Italy. [4] University of Natural Resources and Life Sciences, Department of Forest- and Soil Sciences, Institute of Forest Ecology, Vienna, Austria. [5] Environment Agency Austria, Vienna, Austria. [6] UK Center for Ecology & Hydrology, Penicuik, UK. [7] Chair of Climatology, Institute of Ecology, Technische Universität Berlin, Germany. [8] Wageningen University, Meteorology and Air Quality Section, Wageningen, Netherlands. [9] Dep. Of Meteorology, University of Reading, UK. [10] Institute for Atmospheric and Earth System Research (INAR) / Physics, University of Helsinki. Helsinki Institute of Sustainability Science (HELSUS), University of Helsinki, Finland. [11] Remote Sensing Lab, Institute of Applied and Computational Mathematics, Foundation for Research and Technology Hellas (FORTH), Greece. [12] CMCC Foundation - Euro-Mediterranean Center on Climate Change, Italy.

Heatwaves are becoming more intense and long-lasting due to climate change[1,2]. Europe has experienced an especially strong increase in the duration and magnitude of heatwaves in the last two decades compared to other midlatitude regions[1,3]. Major heatwaves occurred across Europe in 2003, 2010, 2018, 2019, 2021, and 2022[2,4]. The heatwave magnitude was approximately 50% higher between 2012 and 2021 than in the previous decade (2002-2011) and ten times higher than 1950-2001[2,3].

Heat stress accounts for the highest number of premature fatalities of all climate-related hazards in Europe and the United States of America[1,2,5,6]. In the last decade (2010–19), the population exposed to heatwaves in Europe has increased by 57% compared with the previous decade (2000–09)[4]. The escalation in exposure led to an increment of 30 additional deaths per million in heat-related mortality in these last two decades in Europe[4]. A European-wide study quantified the heat-related mortality during the summer of 2022 to be over 60,000, estimating 8,173 cases in Germany, 11,324 in Spain and 18,010 in Italy[7].

Exposure to heat is also associated with adverse physiological health risks such as heat stroke and psychological health effects that can lead to loss of productivity in the workplace, reduction in learning capacity, mental health issues and suicide[8,9]. High-latitude areas are subject to higher rates of heat-related mortality than lower latitudes as the population is less acclimatised and possesses lower thermoregulation capacity[4,10].

The effects of heatwaves and the risk of heat-related mortality for inhabitants of dense settlements are exacerbated by several urban features[11]: i) the complex 3D morphology of the urban landscape, which reduces the bulk albedo, increasing the net (all-wave) radiation at the surface[11]; ii) the anthropogenic heat released from buildings, transportation and human metabolism[12]; iii) the impervious surfaces, which increase heat intensity compared natural areas, because of higher heat and storage capacity of these surfaces to trap and subsequently release more heat, especially at night[11,12]; finally iv) the lack of vegetation, which restricts the cooling capacity during a heat wave event[13]. These urban features are the primary causes of urban heat island (UHI) formation[14]. UHI refers to the phenomenon of built-up areas being significantly warmer than the surrounding rural or greenbelt areas, especially during nighttime, due to these alterations in urban features and land cover[11].

Green infrastructure provides numerous ecosystem services, including a cooling effect via the attenuation of solar radiation by shade and evapotranspiration (ET)[14]. The development of urban green infrastructure (UGI) is therefore one of the best-suited nature-based solutions to mitigate overheating[14–16]. In both extremes of humid (energy-limited) and arid (water-limited) environments, the shade provision of vegetation may contribute more to the cooling service than ET[13,17,18]. Urban greening also helps to mitigate other climate-

related hazards such as droughts and floods as it reduces run-off, favouring soil infiltration to recharge the water table[19]. Therefore, green infrastructures are crucial for improving the well-being of urban residents[7,19]. However, denser urban areas have higher building and impervious fractions, often lacking vegetated areas, limiting the capacity to offer green cooling services to mitigate outdoor heat stress[14,19].

Green cooling should be fairly distributed within a city to promote environmental justice[20]. Although access to green cooling services in urban areas is mostly related to climatic and distributive environmental justice, it is also indirectly associated to energy demand, air pollution and biodiversity injustices[21,22]. Several studies in the US have indicated environmental injustices, showing that lower-income, outdoor workers and certain ethnic groups are subject to a higher risk of heat stress and fatalities[23–25].

Some studies have also shown injustice at the European scale, finding the vulnerability to climate exacerbated for residents in low-income countries[26,27]. Environmental justice studies in European cities have focused on the accessibility and provision of green infrastructure or outdoor recreation[28–30]. However, environmental justice studies that assess the intraurban distribution of cooling services and the population strata more exposed to heat stress remain limited in most European cities[31,32].

Most recent studies assessing heat stress in cities are based on differences in land surface temperature (LST) between urban and rural areas to determine UHI[33]. The standard method of assessing urban heat has recently shifted from air temperature measurements to mainly daytime thermal infrared imagery, which limits investigations to the Surface Urban Heat Island[34]. However, human thermal comfort and well-being are more associated with a combination of radiation, wind speed, air temperature and humidity than LST[16]. Thermal imagery is also limited in spatial and temporal resolution. LST retrieved by remote sensing requires clear-sky conditions, which may limit the availability of images suitable for intraurban analyses during heatwave events[33,34].

A precise assessment of cooling services provided by soil evaporation and plant transpiration is complex to achieve due to the heterogeneity of the urban canopy[14,35,36]. Eddy covariance (EC) flux towers are a widely accepted micrometeorological approach to directly measure the turbulent heat and water fluxes in the atmosphere[37]. Nevertheless, ET is measured by flux towers in very few urban locations over Europe[38,39] and

only allows the assessment of a portion of the heterogeneous urban environment (often a neighbourhood scale footprint). A process-based modelling evaluated by flux towers offers an excellent opportunity to accurately simulate spatially-resolved green cooling services across urban environments[12,40,41].

Green Cooling Service Simulations

This study presents a unique set of indices developed to quantify radiative and evapotranspirative cooling services of greening in urban environments[40]. This novel approach to assessing the exposure to heat stress is based on spatially-explicit simulations of 1) the normalised reduction of the soil skin temperature below the canopy provided by shade (RCoS index) and 2) the normalised daily ET values (ECoS index)[40]. The green cooling services index (GCoS) is the mean value of the RCoS and ECoS subindices. This approach allows for more flexibility in selecting a spatial and temporal resolution suitable for heat stress dynamics in urban environments by using a soil-vegetation-atmosphere process-based model (SVAT)[41]. The final products can be presented at a high spatial resolution (10 m) to support urban planning actions on low cooling areas and at a neighbourhood scale (500 m) to reveal environmental injustices within and between cities.

Environmental justice is assessed by relating outdoor access to green cooling services in 14 major European urban areas from 13 countries. The Functional Urban Areas from the Global Human Settlement provided by the Copernicus Land Monitoring Service were used to define the boundaries of urban areas consistently among countries[42]. The main cities of the urban areas assessed in this study are Amsterdam, Athens, Basel, Berlin, Budapest, Florence, Helsinki, Istanbul, London, Madrid, Paris, Rome, Stockholm and Vienna. The GCoS index was simulated and mapped for each urban area on its hottest day in 2022.

We evaluate to what extent the socioeconomic status of the residents determines local access to green cooling in urban areas and whether intra-urban inequalities correspond to spatial variations in GCoS. Environmental justice was assessed based on standardised socioeconomic indicators such as household income, employment, housing, immigration, and population characteristics extracted from the national census and scaled to neighbourhood level.

Green Cooling Services distribution

Heat stress hazards can greatly vary according to the different microclimates inside a city undergoing a heatwave. The GCoS is a 0-1 index developed to assess the intraurban intensity of the heat stress hazard. Lower GCoS values correspond to higher levels of heat stress. The distribution of GCoS is very distinctive when comparing the different European urban areas. Fig. 1 shows the spatial patterns of the cooling services and the distribution of the two lower quintiles (40%) of the household income for eight selected urban areas. The areas of low cooling services are, in most cases, spread around the centre of the main city of the urban area. GCoS values are higher in the outskirts but also concentrated in some large urban parks close to the main city centres. The spatial distribution of the index is very clustered in most areas (global Moran's I statistic from 0.59 to 0.92), which means that places with high heat stress are concentrated in specific regions of the city.

The 40% lower household income residents are broadly concentrated in central areas of the Functional Urban Areas of Amsterdam, Berlin, Madrid and Vienna. In London and Paris, the lower-income areas are more concentrated in the northeast of the main city centres, whereas in Athens, they are mainly in the western part of the city. In general, the green cooling is more clustered than the distribution of lower-income groups, which is confirmed by the spatial autocorrelation (Moran's I statistics) values for all urban areas except Basel. The bivariate Global Moran's I statistic is negative between GCoS and 40% lowest income for all urban areas (inversely associated). Therefore, the GCoS is likely to be reduced in locations with relatively low income, especially in Amsterdam, Berlin, Paris, and Madrid, which present joint autocorrelation stronger than -0.4.

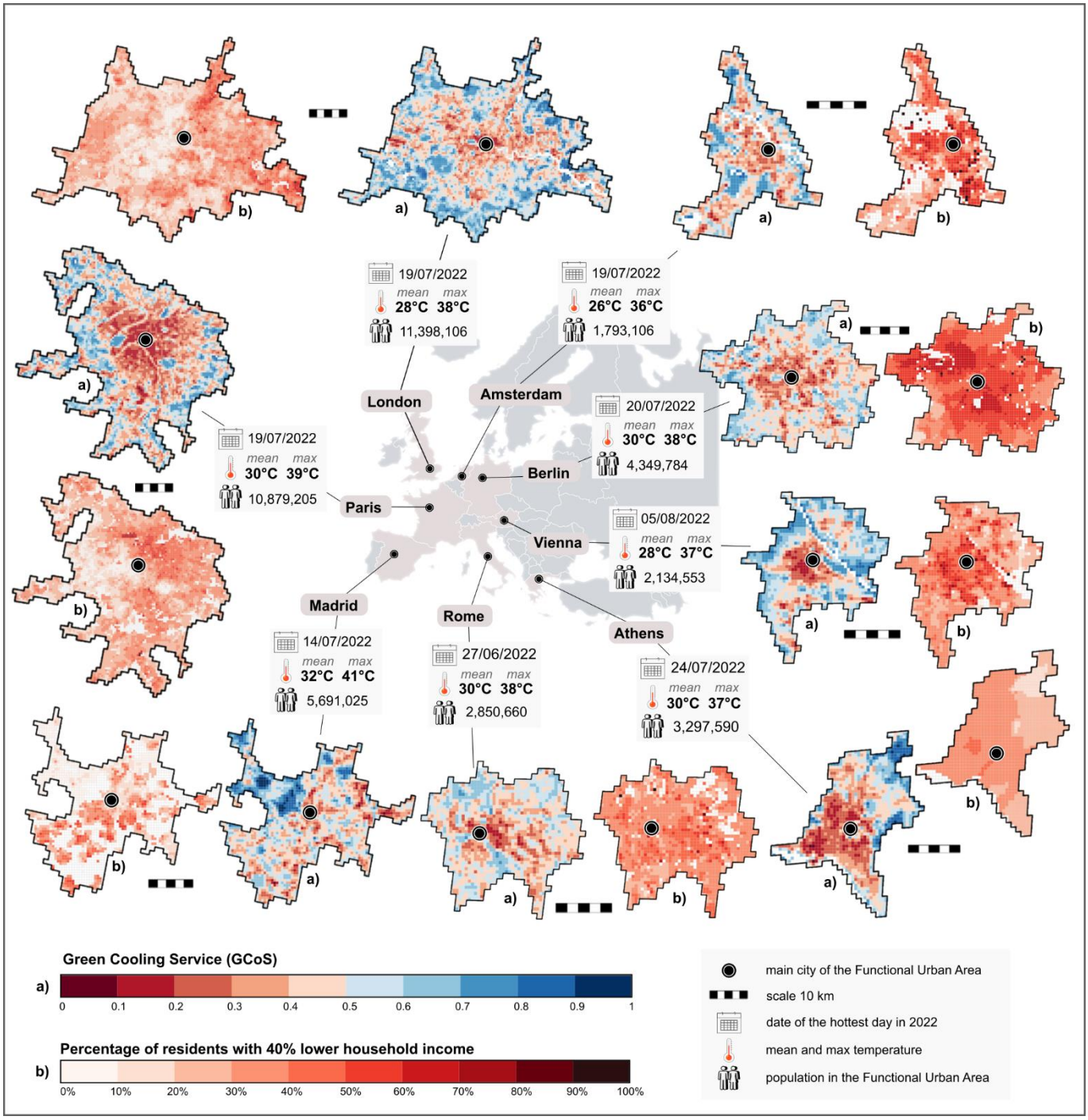

Fig.1: Spatial distribution of the Green Cooling Services index - GCoS during the hottest day of 2022 in the main city (a) and the percentage of residents with 40% lower household income (b) for a selection of studied urban areas. The urban areas and the population estimates are based on the Urban Atlas and the Global Human Settlement Layers, representing the conurbations as Functional Urban Areas rather than administrative city borders. Each map is presented in a 500 m resolution grid and supplied with individual scale bars in km.

It is important to point out that the GCoS values are not directly comparable between the urban areas as they are based relative indices derived from normalised values (e.g. ET) within the city. However, the distribution

shape and the spatial dispersion can show how concentrated the cooling service is in each urban area. For instance, urban areas of Istanbul and Madrid present symmetric distributions with more than half of the locations with GCoS below 0.5, while Florence and Budapest have left-tailed distributions with much higher median values (Fig. 2).

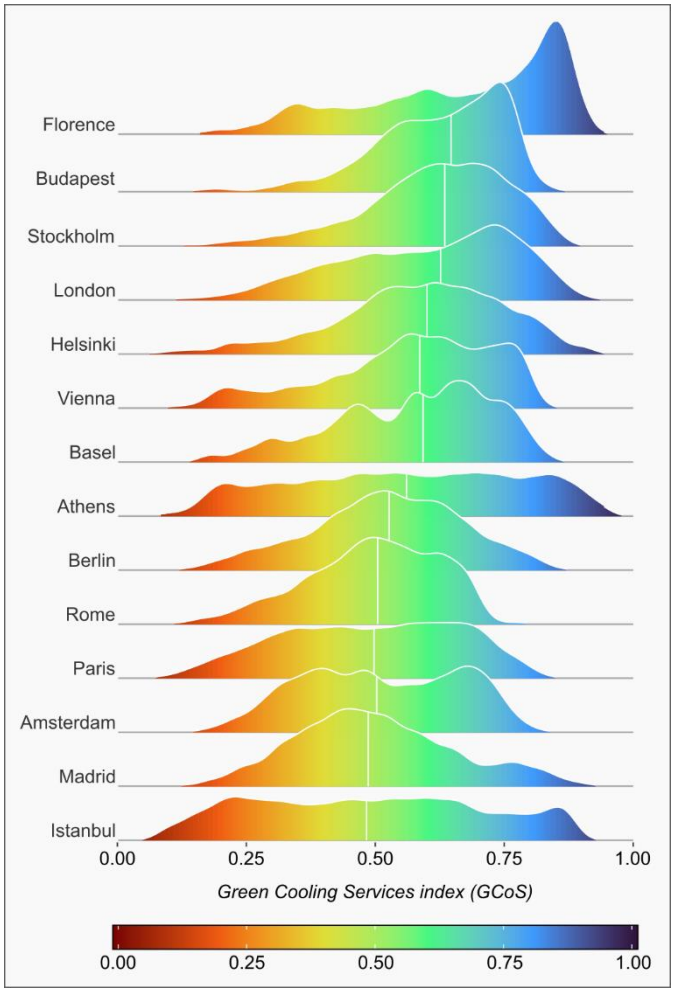

Fig.2: Green Cooling Services index (GCoS) distribution ordered by the median for the 14 studied European urban areas during the hottest day of 2022. Areas with less than ten households were excluded to avoid the influence of big parks or industrial and commercial spaces with nearly no residents.

The population most exposed to heat stress

As we demonstrated, the GCoS is unevenly distributed in the urban areas, and part of the population will be more exposed to a higher risk of heat stress than others. In Fig. 3, we compared the proportions of the population according to four levels of green cooling services in the surroundings of their residences. Only a tiny proportion of the population lives in areas with the highest GCoS (fourth quartile) because they are

located in areas with low impervious fractions and, therefore, fewer buildings. Therefore, there is a strongly inversely proportional relationship between demographic density and the GCoS index (r = -0.62).

When comparing the urban areas, while two-thirds of the Budapest population live in areas with a GCoS index > 0.5, less than 20% of the inhabitants living in urban areas around Amsterdam, Athens, Istanbul, Paris, and Rome reside in areas with a GCoS > 0.5. Greater London has the second lowest proportion of the population in the first quartile of the index (0 to 0.25), far lower than the other metropolitan areas. However, cooling services are still limited here, as nearly 60% of the population lives in areas with an index between 0.25 and 0.50. Only in Helsinki, Budapest, and Stockholm do more than half of the population live in neighbourhoods with GCoS > 0.5.

The GCoS index is calculated to be relative to the highest value of cooling service in each urban area (the lowest is equal to zero). As the highest GCoS often has low demographic density and uneven spatial distribution, a significant proportion of the population tends to live in areas susceptible to heat stress. However, it is necessary to understand the vulnerability and adaptive capacity of the population to propose mitigation actions to reduce the risks and consequences of heat stress exposure.

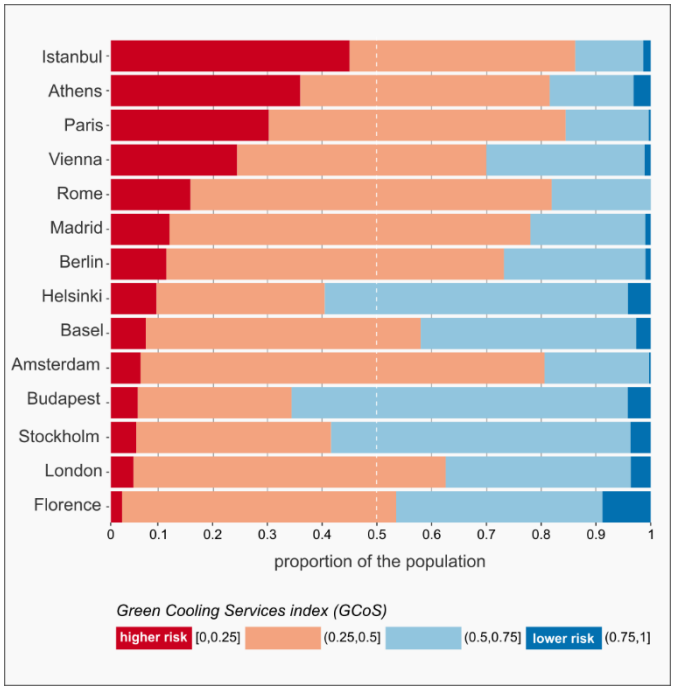

Fig. 3: Proportion of the population per Green Cooling Services index (GCoS) quartiles on the hottest day of 2022 per urban area.

Socioeconomic risk factors for heat exposure

Socioeconomic factors are closely correlated with green cooling services: the correlation between GCoS and the proportion of low-income groups is consistently inversely proportional (negative) to the first and second lowest quintiles and positively correlated with the highest income group (upper quintile) in all studied urban areas (Fig. 4).

The third quintile of income is primarily negative. The fourth quintile depends on the relationship with the national income classes. Capitals such as London, Paris, and Madrid have much higher incomes than the rest of the country, showing negative correlations. In contrast, the opposite relationship is observed in Amsterdam, Vienna, and Berlin. The average purchasing power per capita is mainly positively correlated with GCoS, while unemployment is inversely proportional.

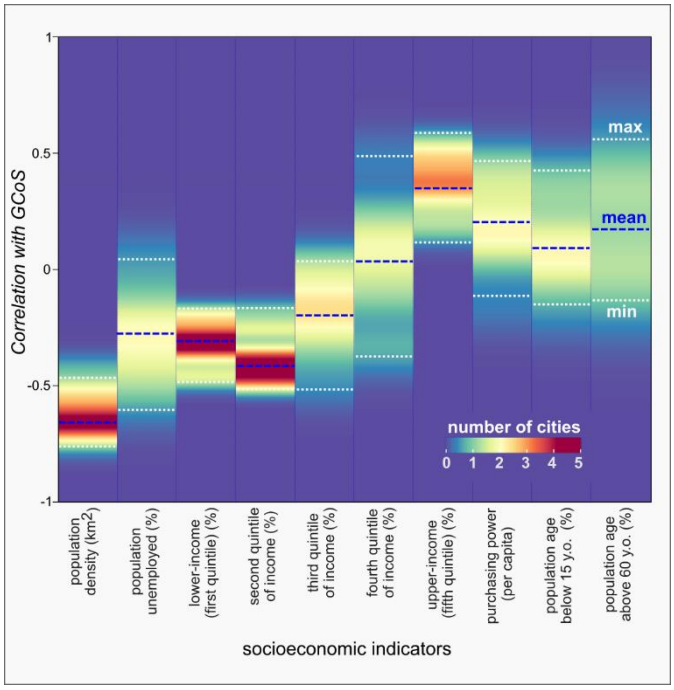

Fig. 4: Number of cities (density) per level of Pearson correlation values between socioeconomic indicators and the Green Cooling Services index (GCoS) across the 14 European urban areas.

The relationship between cooling and the proportion of the population below the age of 15 and above 60 years old is inconsistent among the urban areas. The population over 60 years old is more exposed to cooling on average. However, while Greater London shows a strong positive correlation (0.62), Rome is moderately negatively correlated (-0.19). In contrast, the population under 15 years old is moderately negatively correlated to the GCoS index in London (-0.20), while the opposite relationship occurs in Stockholm and

Budapest (0.36 and 0.40). Although the effects of heatwaves tend to impact both age classes more than the other age groups, the youngest and oldest populations are, in general, less prevalent in areas with high heat stress.

The socioeconomic indicators are clearly clustered into two groups, one that increases access to cooling services and another that aggravates the risk of heat exposure (Fig. 5). There are also similarities among cities influenced by historical factors and background climate, which are illustrated by the patterns in the correlation between the socioeconomic indicators and the cooling index. For instance, the heatmap clusters (i) Berlin, Vienna, Basel, and Paris and (ii) Budapest, Helsinki, and Stockholm. Although the mean values of GCoS were not used to group the urban areas, the clusters also present similar indices. The combination of the indicators, employment, income and purchasing power, clearly shows that European access to green cooling services is not egalitarian.

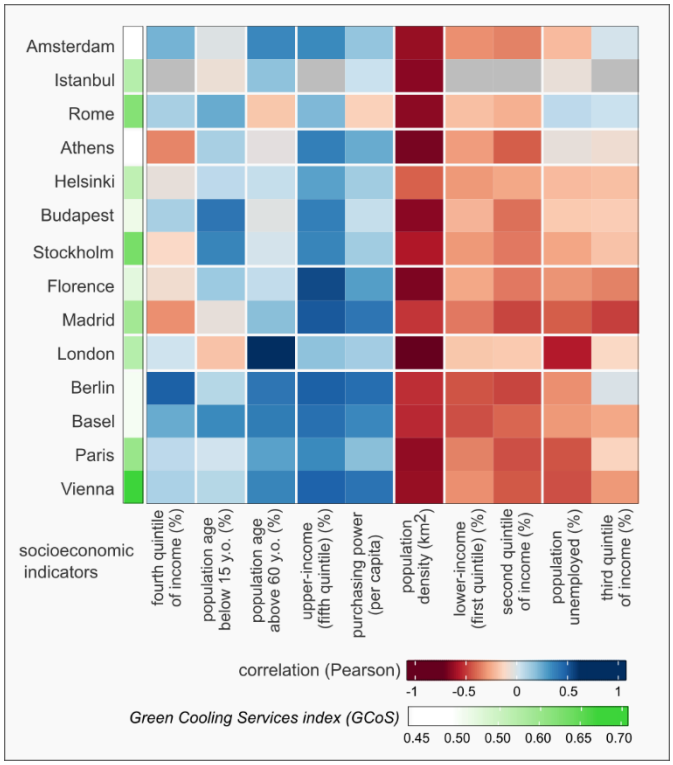

Fig.5: Heatmap of urban areas (rows) and socioeconomic indicators (columns) based on correlation with the Green Cooling Services index (GCoS). The horizontal and vertical white lines represent cluster groups according to dendrograms.

Environmental injustice in European urban areas

Using socioeconomic indicators, this study reveals that environmental injustice regarding heat stress mitigation is widespread across European urban areas. Lower-income and unemployed groups in all selected urban areas have lower access to GCoS than upper-income groups. These differences can be quite substantial: in Greater London, while the index for upper-income groups is, on average, 0.65, the value for the unemployed population is 0.51. In Madrid, the upper-income quintile has, on average, 0.1 higher GCoS (20% higher) than the 40% lower-income group.

In addition to household income, housing and immigration status are strongly related to access to cooling services from green spaces (Fig. 6). For instance, homeowners have a cooling index 0.1 higher than tenants in Berlin. Moreover, home characteristics, such as multifamily households, detached houses, number of rooms, or home market prices, affect access to cooling services. These attributes serve as a proxy for the socioeconomic characteristics of the neighbourhood rather than the influence of the building structure on cooling. Areas with detached houses have higher cooling services in Amsterdam ($r = 0.44$). In Madrid, sales prices of homes are positively correlated with cooling services ($r = 0.45$), while homes with five rooms or more are strongly correlated with the index in Paris ($r = 0.62$).

Overall, 22% of the population in the urban areas surveyed are exposed to a cooling index lower than 0.25, with more than half residing in regions with GCoS between 0.25 and 0.50. Around three out of four people live in regions with inadequate levels of cooling (< 0.5), with one-third of those being in vulnerable age groups (under 15 or over 60 years old).

Although age groups showed an inconsistent relationship with access to cooling, other factors such as immigrant origin play a crucial role. In the urban areas of Berlin, Paris and Madrid, immigrants account for around 10% of all households. Among immigrants, the GCoS average is below 0.5 in the Paris and Berlin urban areas (0.46 and 0.49), up to 0.09 lower than that accessed by nationals (18% and 19%). The lowest income quintile and the proportion of immigrants are closely associated in both areas according to the bivariate global Moran's I statistic (0.42 and 0.55, respectively). The difference between immigrants and

nationals was generally lower in Madrid, but the cooling access was found to be further reduced among immigrants from Africa and South America.

Despite significant historical and economic differences, underprivileged residents mainly live in areas lacking green cooling services in most urban areas. The exception is Rome, which presents a relatively lower correlation between GCoS and income than other areas. This is explained by a much weaker spatial autocorrelation for the lowest household income (0.35) than for GCoS (0.78), resulting in a low bivariate global Moran's I (-0.14).

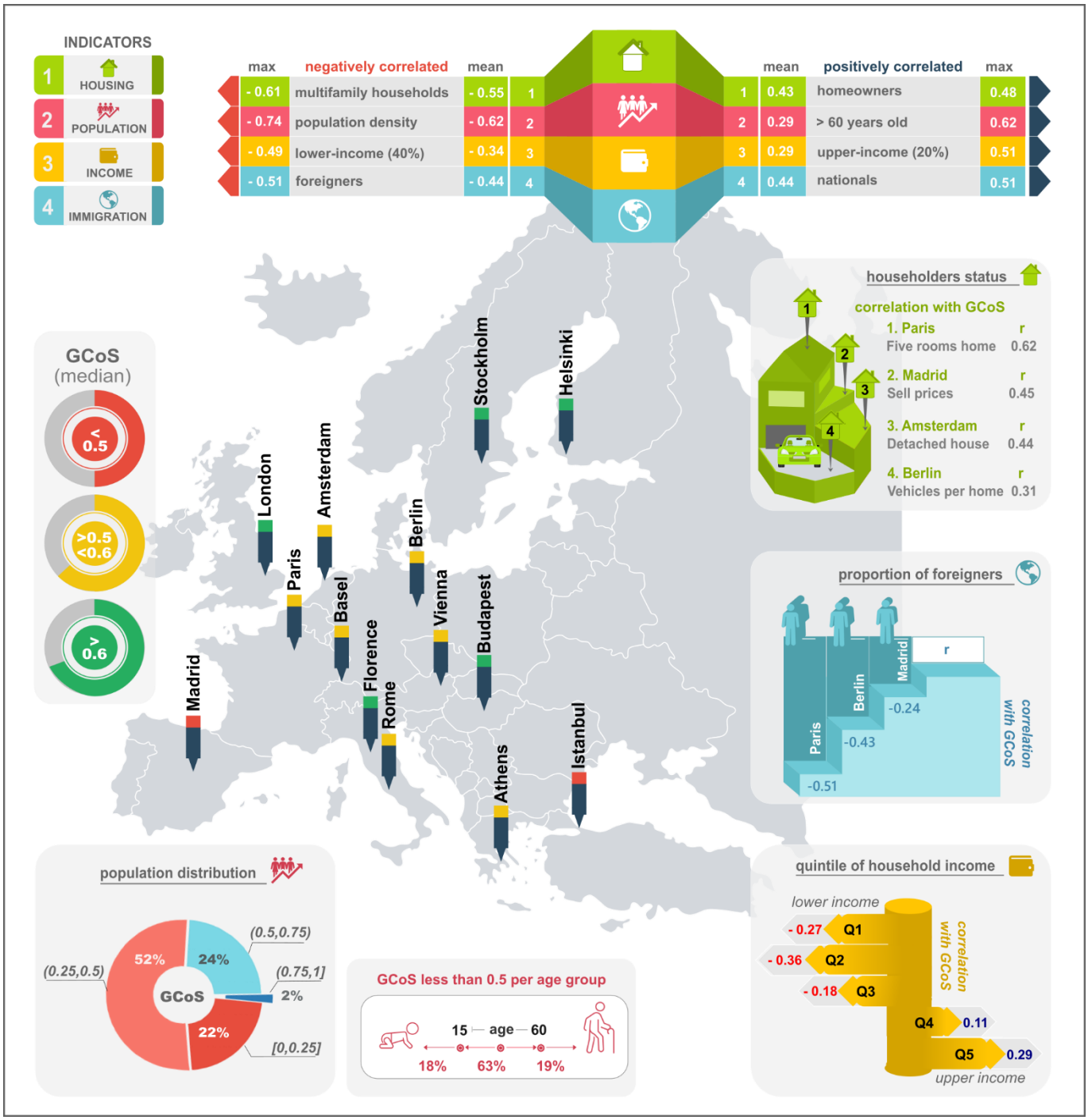

Fig.6: Infographic presenting the relationship between the Green Cooling Services (GCoS) index and the indicators of housing, population, income, and immigration.

Discussion

Our study revealed environmental injustice concerning green cooling services in 14 European urban areas. This study clearly warns that vulnerability to climate change is not only exacerbated for residents of low-income countries but also for low-income and underprivileged urban residents of wealthy European regions[28]. Intraurban inequalities are a well-known fact in large cities. In Europe, vulnerable residents are not primarily concentrated in suburban areas but in run-down central areas with lower green cooling services[43].

Most studies assessing environmental inequality in heat stress were based on Gross Domestic Product (GDP) at the national level, overlooking subnational and intraurban variations in inequality[2,27]. We overcome this limitation by assessing environmental justice regarding access to green cooling services based on standardised census socioeconomic indicators in the functional areas of major European cities at the neighbourhood scale.

Furthermore, the methodology of this study can be used to prioritise intraurban areas with low cooling services and high population vulnerability to promote mitigation actions targeting environmental injustice. However, interventions to mitigate urban heat by incorporating green spaces will most likely displace lower-income populations if not well planned (green gentrification)[44,45].

Revitalising an area often increases property values, facilitating the migration of affluent people searching for climate-resilient greener regions to live in[44–46]. Therefore, overheating mitigation actions should avoid large localised projects and promote spatially-distributed measures to improve green cooling. Otherwise, green spaces will not promote environmental justice but rather become an agent of further aggravation of injustice[20]. For instance, urban planning measures can aim for an even distribution of tree cover in all regions of a city to match upper-class and tourist areas.

Environmental injustice epitomises unfairness, as the groups that contribute the least to climate change are often the most affected by its impacts[44,45]. The concept of environmental justice originated over 30 years ago

but has increased in relevance, particularly since the unprecedented rise in mean temperatures due to climate change[47]. Our study has focused on distributive justice, meaning that environmental benefits and responsibilities should be proportionately and fairly shared among all population groups. However, recognitional and procedural justice, being based on acquiring local knowledge, respecting diversity, and engaging communities with shared planning and decision-making processes are crucial to promoting distributive justice[20,22].

Our results offer insights with respect to climate migration. The phenomenon of human mobility due to the direct and indirect effects of climate change, such as flooding or low agricultural yields, is a growing concern which particularly affects the less affluent regions of the world. The spatial association between GCoS, lower income, and foreigners' proportion for Paris and Berlin shows that climate immigrants are more likely to end up again in underprivileged areas, where the local provision of green cooling is lower.

Although our study focuses on the injustices of outdoor green cooling, housing and income inequalities observed in the cities are also reflected in indoor cooling. Hence, those residents most exposed to heat stress are also more vulnerable due to their limited capacity to implement indoor cooling measures. The most affected groups by UHI effects are least able to afford air conditioning (active cooling) and less flexible to adapt their homes as tenants (passive cooling)[4,46].

The indoor thermal comfort during heat waves can also vary significantly according to the characteristics of the home (position, material, cooling systems)[9,32]. Our study shows that neighbourhoods with detached houses are associated with higher outdoor green cooling services. Lower-income households are more likely to live in small, overcrowded, poorly-ventilated, or poorly-insulated homes[31]. With the ongoing increase in housing demand and rental prices in large European cities, the possibility of choosing a home with high thermal comfort is a privilege for few.

Our methodology is based on green cooling provided by latent heat flux and radiative blocking simulated by soil-vegetation-atmosphere interaction, while most heat stress studies rely on LST from thermal images. Both approaches underscore vegetation as the most relevant factor in determining intraurban heat intensity. However, shifting from emphasising surface characteristics such as albedo and heat capacity in LST studies

(mainly focusing on sensible heat flux) to focusing on evapotranspirative and radiative cooling of greening in our approach presents several advantages: 1) If the albedo of the dominant buildings is lower than that of the local vegetation, LST may be higher in the rural area than the urban (e.g. Matera in Italy[13]); 2) Our approach is flexible in selecting the spatial and temporal resolution most suitable for the city scale and the heatwave period as it does not rely on the availability of thermal images; and 3) The green cooling is explicitly modelled to address heat stress while LST lacks a mechanism to separate various confounding factors such as background temperatures and surface materials.

Our approach presents some limitations related to the availability and resolution of the model inputs to simulate green cooling. For instance, the spatial resolution of the LAI product (300 m) is much coarser than the vegetation height and impervious fraction (10 m), which can slightly underestimate fragmented vegetation such as small private gardens and street vegetation. During drought events or in water-limited regions (e.g. semi-arid), low moisture and high evaporative demand may require more specific plant trait parameters for model calibration[48]. For instance, the stomatal conductance and soil moisture model parameters were kept constant in time and space (default value). However, our main aim was to associate intraurban variations in GCoS with socioeconomic factors rather than reaching a higher model accuracy. Also, site-specific constant parameters would not alter the relationships found within each city.

Furthermore, coastal areas and regions with significant water bodies, like Athens, Helsinki, and Amsterdam, receive blue cooling services from evaporation[49,50]. Although blue cooling is partially neglected in our index, areas near channels or sea coastlines often present high market values, as found in Helsinki[51]. Incorporating the proximity to water bodies may exacerbate the injustices observed in this study further.

Although our results mainly focus on large urban areas, the accuracy in medium-sized cities (e.g. Basel) or residential areas (e.g. Berlin) indicates that the method also suits small cities. The spatially-limited footprints of the EC observations provide neighbourhood-level verification of the modelling approach across a variety of urban landscapes. Nonetheless, the patterns of green cooling and level of environmental justice in smaller urban areas still warrants further investigation. Furthermore, changes in urban area definition (i.e. extent) may alter whether environmental injustice is concentrated in central areas or the surroundings, but the

injustice in cooling would remain. We assessed environmental justice in European cities using Functional Urban Areas. While administrative borders may be more meaningful for local governments, the high-resolution maps of green cooling can also be utilised to support local urban planning and heat mitigation at the city-level.

Despite the above-mentioned limitations, our method, which relies exclusively on open-access data, was shown to be robust and suitable to support heat stress mitigation, providing sufficient accuracy when compared to ET (i.e. turbulent latent heat flux) measurements from flux towers. Heatwaves have hit Europe hard, and current climate change scenarios indicate they will increase in intensity and length. Urban areas expose residents to more extreme temperatures due to the UHI effect and hold most of the continent's population. Urban high-latitude regions are exposed to solar radiation for extended periods during summer days, and short nights offer little relief in the surface and air temperatures, especially in densely built-up areas. Therefore, nature-based mitigation actions focusing on urban greening are crucial to reduce the escalation of heat-related deaths in Europe.

The proposed method allows further simulations of cooling services under scenarios of land cover conversion (e.g. new UGI) and climate change (e.g. water scarcity, rising temperatures). The developed approach could support the implementation of urban Nature Based Solutions (NBS) and monitoring programs such as the *Mission on 100 Climate-Neutral and Smart Cities by 2030* from Horizon Europe. Furthermore, environmental justice can be promoted by assessing, at a neighbourhood scale, the population characteristics according to the level of green cooling services provided. The revealed environmental injustice affects a significant proportion of unprivileged minorities. As these groups are concentrated in densely populated areas, action to improve their conditions would benefit a significant proportion of urban residents.

References

1. Rousi, E., Kornhuber, K., Beobide-Arsuaga, G., Luo, F. & Coumou, D. Accelerated western European heatwave trends linked to more-persistent double jets over Eurasia. *Nat. Commun.* **13**, 1–11 (2022).
2. Alizadeh, M. R. *et al.* Increasing Heat-Stress Inequality in a Warming Climate. *Earth's Futur.* **10**, 1–11 (2022).
3. Lhotka, O. & Kyselý, J. The 2021 European Heat Wave in the Context of Past Major Heat Waves. *Earth Sp. Sci.* **9**, 1–12 (2022).

4. van Daalen, K. R. *et al.* The 2022 Europe report of the Lancet Countdown on health and climate change: towards a climate resilient future. *Lancet Public Heal.* **7**, e942–e965 (2022).
5. Uejio, C. K. *et al.* Intra-urban societal vulnerability to extreme heat: The role of heat exposure and the built environment, socioeconomics, and neighborhood stability. *Heal. Place* **17**, 498–507 (2011).
6. Chakraborty, T., Hsu, A., Manya, D. & Sheriff, G. Disproportionately higher exposure to urban heat in lower-income neighborhoods: A multi-city perspective. *Environ. Res. Lett.* **14**, 105003 (2019).
7. Ballester, J. *et al.* Heat-related mortality in Europe during the summer of 2022. (2023) doi:10.1038/s41591-023-02419-z.
8. García-León, D. *et al.* Current and projected regional economic impacts of heatwaves in Europe. *Nat. Commun.* **12**, 1–10 (2021).
9. Buchin, O., Hoelscher, M. T., Meier, F., Nehls, T. & Ziegler, F. Evaluation of the health-risk reduction potential of countermeasures to urban heat islands. *Energy Build.* **114**, 27–37 (2016).
10. Gronlund, C. J. Racial and Socioeconomic Disparities in Heat-Related Health Effects and Their Mechanisms: a Review. *Curr. Epidemiol. Reports* **1**, 165–173 (2014).
11. Oke, T. R. The urban energy balance. *Prog. Phys. Geogr.* **12**, 471–508 (1988).
12. Chrysoulakis, N. *et al.* Urban energy exchanges monitoring from space. *Sci. Rep.* **8**, 1–8 (2018).
13. Manoli, G. *et al.* Magnitude of urban heat islands largely explained by climate and population. *Nature* **573**, 55–60 (2019).
14. Wong, N. H., Tan, C. L., Kolokotsa, D. D. & Takebayashi, H. Greenery as a mitigation and adaptation strategy to urban heat. *Nat. Rev. Earth Environ.* **2**, 166–181 (2021).
15. Schwaab, J. *et al.* The role of urban trees in reducing land surface temperatures in European cities. *Nat. Commun.* **12**, 1–11 (2021).
16. Ward, K., Lauf, S., Kleinschmit, B. & Endlicher, W. Heat waves and urban heat islands in Europe: A review of relevant drivers. *Sci. Total Environ.* **569**–**570**, 527–539 (2016).
17. Naserikia, M., Hart, M. A., Nazarian, N. & Bechtel, B. Background climate modulates the impact of land cover on urban surface temperature. *Sci. Rep.* **12**, 1–15 (2022).
18. Yu, Z., Xu, S., Zhang, Y., Jørgensen, G. & Vejre, H. Strong contributions of local background climate to the cooling effect of urban green vegetation. *Sci. Rep.* **8**, 1–9 (2018).
19. Marando, F. *et al.* Urban heat island mitigation by green infrastructure in European Functional Urban Areas. *Sustain. Cities Soc.* **77**, 103564 (2022).
20. Kato-huerta, J. & Geneletti, D. Environmental justice implications of nature-based solutions in urban areas : A systematic review of approaches , indicators , and outcomes. *Environ. Sci. Policy* **138**, 122–133 (2022).
21. Rockström, J. *et al.* Safe and just Earth system boundaries. **619**, (2023).
22. Gupta, J. *et al.* Earth system justice needed to identify and live within Earth system boundaries. **6**, 630–638 (2023).
23. Stewart, I. D. *et al.* Time Evolution of the Surface Urban Heat Island. *Earth's Futur.* **9**, (2021).
24. McDonald, R. I. *et al.* The tree cover and temperature disparity in US urbanized areas: Quantifying the association with income across 5,723 communities. *PLoS One* **16**, 1–27 (2021).
25. Mitchell, B. C. & Chakraborty, J. Exploring the relationship between residential segregation and thermal inequity in 20 U.S. cities. *Local Environ.* **23**, 796–813 (2018).
26. Zhang, J. *et al.* Inequality of global thermal comfort conditions changes in a warmer world. *Earth's Futur.* (2023) doi:10.1029/2022ef003109.
27. Krummenauer, L., Costa, L., Prahl, B. F. & Kropp, J. P. Future heat adaptation and exposure among urban populations and why a prospering economy alone won't save us. *Sci. Rep.* **11**, 1–14 (2021).
28. Silva, C. D. S. & Panagopoulos, T. Environmental Justice in Accessibility to Green. (2018) doi:10.3390/land7040134.
29. Kabisch, N. & Haase, D. Landscape and Urban Planning Green justice or just green ? Provision of urban green spaces in Berlin ,. *Landsc. Urban Plan.* **122**, 129–139 (2014).
30. Suárez, M. *et al.* Environmental justice and outdoor recreation opportunities : A spatially explicit assessment in Oslo metropolitan area , Norway. *Environ. Sci. Policy* **108**, 133–143 (2020).
31. Sandholz, S., Sett, D., Greco, A., Wannewitz, M. & Garschagen, M. Rethinking urban heat stress: Assessing risk and adaptation options across socioeconomic groups in Bonn, Germany. *Urban Clim.* **37**, (2021).
32. Hölzl, S. E., Veskov, M., Scheibner, T., Le, T. T. & Kleinschmit, B. Vulnerable socioeconomic groups are disproportionately exposed to multiple environmental burden in Berlin - implications– for planning. *Int. J. Urban Sustain. Dev.* **13**, 334–350 (2021).
33. Zhou, D. *et al.* Satellite remote sensing of surface urban heat islands: Progress, challenges, and perspectives. *Remote Sens.* **11**, 1–36 (2019).
34. Parlow, E. Regarding some pitfalls in urban heat island studies using remote sensing technology. *Remote Sens.* **13**, (2021).

35. Rahman, M. A. *et al.* Spatial and temporal changes of outdoor thermal stress: influence of urban land cover types. *Sci. Rep.* **12**, 1–13 (2022).
36. Souverijns, N. *et al.* Urban heat in Johannesburg and Ekurhuleni, South Africa: A meter-scale assessment and vulnerability analysis. *Urban Clim.* **46**, (2022).
37. Schmutz, M., Vogt, R., Feigenwinter, C. & Parlow, E. Ten years of eddy covariance measurements in Basel, Switzerland: Seasonal and interannual variabilities of urban CO 2 mole fraction and flux. *J. Geophys. Res. Atmos.* **121**, 8649–8667 (2016).
38. Matthews, B. & Schume, H. Tall tower eddy covariance measurements of CO2 fluxes in Vienna, Austria. *Atmos. Environ.* **274**, 118941 (2022).
39. Nicolini, G. *et al.* Direct observations of CO2 emission reductions due to COVID-19 lockdown across European urban districts. *Sci. Total Environ.* **830**, (2022).
40. Rocha, A. D., Vulova, S., Meier, F., Förster, M. & Kleinschmit, B. Mapping evapotranspirative and radiative cooling services in an urban environment. *Sustain. Cities Soc.* **85**, 104051 (2022).
41. Duarte Rocha, A., Vulova, S., Van Der Tol, C., Förster, M. & Kleinschmit, B. Modelling hourly evapotranspiration in urban environments with SCOPE using open remote sensing and meteorological data. *Hydrol. Earth Syst. Sci.* **26**, 1111–1129 (2022).
42. Frye, C., Nordstrand, E., Wright, D. J., Terborgh, C. & Foust, J. Using classified and unclassified land cover data to estimate the footprint of human settlement. *Data Sci. J.* **17**, 1–12 (2018).
43. Lapola, D. M., Braga, D. R., Di Giulio, G. M., Torres, R. R. & Vasconcellos, M. P. Heat stress vulnerability and risk at the (super) local scale in six Brazilian capitals. *Clim. Change* **154**, 477–492 (2019).
44. Kotsila, P. & Anguelovski, I. Justice should be at the centre of assessments of climate change impacts on health. *Lancet Public Heal.* **8**, e11–e12 (2023).
45. Anguelovski, I. *et al.* Why green 'climate gentrification' threatens poor and vulnerable populations. *Proc. Natl. Acad. Sci. U. S. A.* **116**, 26139–26143 (2019).
46. Santamouris, M. & Kolokotsa, D. On the impact of urban overheating and extreme climatic conditions on housing, energy, comfort and environmental quality of vulnerable population in Europe. *Energy Build.* **98**, 125–133 (2015).
47. Horne, Y. O. Van *et al.* An applied environmental justice framework for exposure science. (2022) doi:10.1038/s41370-022-00422-z.
48. Cuthbert, M. O., Rau, G. C., Ekström, M., O'Carroll, D. M. & Bates, A. J. Global climate-driven trade-offs between the water retention and cooling benefits of urban greening. *Nat. Commun.* **13**, (2022).
49. Burkart, K. *et al.* by Vegetation (Urban Green) and Proximity to Water (Urban Blue): **124**, 927–934 (2016).
50. Quaranta, E., Dorati, C. & Pistocchi, A. Water, energy and climate benefits of urban greening throughout Europe under different climatic scenarios. *Sci. Rep.* **11**, 1–10 (2021).

Methods

Modelling and validation

The SVAT model used in ET and soil temperature simulations is the Soil-Canopy-Observation of Photosynthesis and Energy Fluxes (SCOPE)[52,53]. SCOPE is a process-based approach integrating a plant canopy radiative transfer model with heat fluxes and energy balance[41,52]. The SCOPE simulations at 300 m resolution are then adjusted to the unsealed fraction (10 m) in the second stage using the Imperviousness Density 2018 product provided by the Copernicus Land Monitoring Service[54]. This product is a Europe-wide high-resolution (10 m) layer derived from Sentinel-2 images that quantify the sealing density in the range of

0-100% for the period from 2017 to 2019. A series of imperviousness datasets are available from 2006 to 2018, updated on a three-year basis for new artificially sealed areas.

The two-stage approach relying on the SCOPE model to predict urban ET was previously applied in a case study in Berlin, Germany[41]. The method was adapted here to utilise open-access input data available for all of Europe, such as meteorological forcing variables and remote sensing-based vegetation parameters. The use of open-access data makes the method reproducible and easily updatable.

Among many plant trait parameters available in SCOPE, Leaf Area Index (LAI) and canopy height (hc) were input for each pixel using remote sensing products (see Extended Data Tab.1). The canopy height is a 10 m resolution raster from ETH Global Canopy Height 2020 product[55], while the LAI product is a 10-day and 300 m resolution dataset from Copernicus Global Land Service[56]. Despite the relatively coarser spatial resolution of the LAI product (300 m) compared to vegetation height and impervious fraction (10 m), the Copernicus LAI product is a consolidated time series dataset globally available. The 10-day temporal resolution captures the plant phenology during the year well, which varies significantly across latitudes and vegetation types. Combining a high-temporal-resolution LAI 300 m product with a finer spatial resolution and higher accuracy product locally available could reduce uncertainties in fragmented urban vegetation.

ET and soil temperature were simulated hourly at a 300 m resolution for the hottest day of 2022 for each urban area in SCOPE. The resolution of the simulations was constrained to 300 m based on the LAI raster resolution. However, the final product was downscaled to 10 m using a surface sealing fraction raster in the second modelling stage.

The hourly meteorological forcing datasets are collected from the atmospheric reanalysis (ERA5)[57] of the European Centre for Medium-Range Weather Forecasts (ECMWF) produced by the Copernicus Climate Change Service (C3S). Hourly air temperature, relative humidity, air pressure, wind speed, incoming shortwave, and longwave radiation were used as model inputs (see Extended Data Tab. 1).

The model accuracy was evaluated by comparing the ET simulation (predicted) and turbulent latent heat flux observations from ten eddy covariance (EC) towers[39] located in Amsterdam (NL), Basel (CH)[37], Berlin (DE)[40,41,58,59], Heraklion (GR)[60], Helsinki (FI)[61,62], Florence (IT), London (UK)[63,64], and Vienna (AT)[38]. In

Basel and Berlin, there are urban EC towers at two locations. The EC datasets were standardised and fully corrected[39]. The towers are located in different temperate and continental Köppen climates classes, and cover a vast range of urban landscapes. Therefore, it is assumed that the model performance can be extrapolated for the urban areas of Paris, Athens, Madrid and Rome, for which no EC data were available.

The period of observed ET (EC data) from 2019 to 2021 was used to assess model performance, depending on the availability in each tower location. The input parameters to simulate ET in the source area around the EC towers (90% contribution) were extracted hourly from the 10 m grids using footprint modelling (i.e. Kormann and Meixner (2001)).

The modelled source areas (footprints) and the ET observations in urban environments may present high uncertainty depending on micrometeorological conditions, measurement height and the surface roughness around the EC tower (errors up to 20-30% in some conditions)[61]. Furthermore, random errors, as well as divergence between surface and turbulent fluxes, must be considered when comparing modelled fluxes to EC measurements. Nonetheless, EC measurements are likely the best available data to evaluate simulations of urban ET due to the spatiotemporal resolution and coverage of the observations.

The coefficient of determination (R^2) between predicted and observed ET varies from 0.21 to 0.82, while the RMSE varies from 0.018 to 0.062 mm h^{-1} (see Extended Data Tab.2 for more details about the metrics per tower). The model accuracy in Berlin and Basel is high for urban ET (i.e. latent heat flux) compared to the literature[65]. The relative bias (rbias) is negative in most cases, even excluding up to 24 hours after rainfall events. The negative bias occurs because, particularly with wet surfaces in winter, the model underestimates ET as intercepted precipitation and anthropogenic sources are neglected. Moreover, urban models tend to underestimate EC measurements of latent heat fluxes even in the summer period[65]. As this study focuses on extreme heatwaves, the effect of interception loss can be considered negligible.

The Extended Fig.1 shows that the predicted ET per hour (24h) agrees quite well with the observed data during the summer (especially July). R^2 is relatively high, ranging from 0.51 to 0.93. Most of the sites observe ET values significantly above zero at night during the entire year, diverging from the simulation, which assumes negligible soil evaporation and plant transpiration in this period. Moreover, the

meteorological forcing data do not capture the UHI and the building heat capacity effects on the night air temperatures. Therefore, nighttime values are the most responsible for the relative bias in the results. The EC towers in London and Vienna are installed at 190- and 144 m height, respectively, increasing the source area and, therefore, the uncertainties of the footprints used for validation[38]. Although our focus is on evapotranspiration and soil temperature, other terms of the energy balance, such as the turbulent sensible heat and the net all-wave radiation, presented strong agreement between observed and predicted values (not shown).

Climatological impacts can be assessed by simulating stress-induced reductions in stomatal conductance due to soil moisture and meteorological scenarios (e.g. air temperature or relative humidity). Pixel level stomatal parameter and soil moisture content can be supplemented as hourly model input to address different climates, soil properties and vegetation types. However, such implementation may be restricted in heterogeneous urban areas by the lack of available spatiotemporal data to adequately parameterise the simulations. However, an optimised site-specific constant for stomatal and soil moisture parameters could be adjusted to represent the entire area and period.

Simulated ET with default parameters may overestimate GCoS over water stress conditions where irrigation is not supplemented[18,66]. Sensitivity analysis per urban area could be performed to optimise some important SCOPE parameters to increase prediction accuracy or explore future scenarios, as achieved in Berlin's case[40,41]. This approach could also be applied to simulate impacts on the cooling service when new green spaces are created. For that, the model should be calibrated with the characteristics of the proposed vegetation. Testing the effect of climatological factors such as low precipitation (drought) or rising temperatures on cooling services is also possible[40].

Green Cooling Services Index GCoS

The green cooling services index (GCoS) is derived from two subindices representing evapotranspirative and radiative cooling[40]. The contribution of each subindex will strongly depend on the vegetation parameters. While canopy height increases RCoS more because it favours shading, LAI benefits ET slightly more as it represents the volume of green leaves available for photosynthesis. Further investigation is needed to

determine if the subindices should have equal weight in the GCoS, which probably will depend on whether the environments are energy- or water-limited.

The evapotranspirative cooling service index (ECoS) is calculated per pixel based on the sum of hourly ET simulations of a 24 hour-period using the SVAT model and corrected based on the impervious surface. The ECoS is normalised by the daily ET range of each urban area to preserve the background conditions, considering the minimal possible ET value to be zero for all urban areas.

The radiative cooling service index (RCoS) is derived from skin soil temperature (Ts_{ave} output), which is modelled based on vegetation characteristics such as canopy height and LAI. The index is designed to capture the differences between shaded and non-shaded vegetated areas (under plant canopy) without considering the urban canopy (shade from buildings). Therefore, we assume only the horizontal fraction of imperviousness without considering building height (3D structure) and its effects on wind speed (street canyons) or shading.

The RCoS index for each pixel is also normalised by the range, using the maximum and minimum soil temperature simulated in the locations during 24 hours. The result is multiplied by the non-impervious fraction to penalise non-vegetated areas using the degree of imperviousness (2018), a 10-m resolution raster with a sealing degree ranging from 0-100%. The impervious fraction was reduced by 10% to account for small gardens and bare soil that are neglected by the 10 m resolution of the imperviousness maps. Water bodies were considered as non-impervious, and irrigation was not included in this study.

The two subindices are averaged to derive the GCoS. All indices vary between 0 and 1, where one represents the highest cooling service and zero represents no green cooling services. The final products are daily maps of cooling services at a 10 m resolution (Extended Data Fig. 2). Further descriptions of the method to simulate the cooling services indices can be found in the original publications[40,41].

Urban areas and socioeconomic indicators

The locations were selected according to the following criteria: 1) European cities with available urban EC tower measurements, and 2) European capitals with more than one million inhabitants without EC towers but in a Köppen classification region covered by EC data. The exceptions are Kyiv and Moscow because

they are not included in the Copernicus Imperviousness Density product. Istanbul (a non-capital without EC data) was included as it represents the most populous European city.

Human settlement borders were selected to compare different countries' main continuous urban fabrics instead of political and administrative boundaries. The extension of these locations was defined based on the Functional Urban Areas provided by the Global Human Settlement Layer (GHSL-FUA) supplied by the European Commission (Copernicus Emergency Service)[67]. The limits of the conurbations may conglomerate multiple cities (or towns) based on criteria such as commuting time, but for simplification, we named the urban areas using the best-known main city.

In some cases, the Urban Centre Database (R2019A) GHSL-based boundaries are mostly restricted to the city limits, such as the case of Berlin, Germany, the largest urban population in Europe. However, in other cases, the GHSL area is spread into hundreds of different municipalities, as is the case for the surroundings of Paris and London, the most populated conurbations in Europe after Moscow and Istanbul. Only urban green spaces are considered. For instance, a significant part of the urban forest of Berlin is outside of the city boundaries and not represented in the GCoS distribution. Thus, mainly UGI that contributes to heat stress reduction for urban residents is considered.

The cooling services and the socioeconomic indicators were compared at a resolution of approximately 500 m using a regular grid to guarantee similar characteristics among all the different countries and functional urban areas. The high-resolution GCoS maps were aggregated to align with the socioeconomic indicators at an approximated neighbourhood scale. This approach avoids averaging sizes and different definitions of neighbourhoods across countries that could mask or introduce bias to the comparative analysis.

The socioeconomic indicators are based on a European-wide standardised national census. The *GeoEnrichment* service from the Esri ArcGIS Pro was used to redistribute the demographic and socioeconomic variables from a granular point dataset to a regular grid of 500 m (so-called neighbourhood scale)[42]. The granular points were distributed in space by the providers considering the location likelihood of being a settlement (~75 m city block) using road intersections and Landsat 8 satellite imagery.

The socioeconomic data are standardised variables for all EU countries provided by the ArcGIS *Living Atlas of the World* (sourced by Esri and Michael Bauer Research GmbH). More detailed housing and migration indicators were available on the same platform only for France, Germany, Spain, and The Netherlands (see "Data Availability"). Although the standardised indicators are not open-access, the original census data are freely available for each country separately.

After extracting the point-based demographic and socioeconomic variables to a 500 m regular grid, a minimum of ten homes per pixel was established as a threshold when comparing the indicators with the GCoS index. This procedure avoids the influence of small sample sizes on the correlation between the indicators and the cooling index (significance tests and intervals of confidence for all indicators per urban areas is available in the Supplementary Information, Table 1).

Most of the indicators were discrete variables such as the number of residents or households and, therefore, could be summed up to grid-level values. However, to avoid the aggregation effect (averaging averages or percentages), other, continuous variables (e.g. purchasing power) were averaged at the pixel-level and subsequently weighted by the number of households per pixel. For instance, in the case of the purchasing power indicator, as upper-income groups generally live in areas with lower population density than lower-income groups, simple pixel averages would inflate their weight in the analysis.

Data analyses

Exploratory analyses were performed to demonstrate the relationship between socioeconomic factors and the simulated green cooling services. Pearson's correlation with socioeconomic indicators was used to show the association of vulnerable households with areas of low cooling service. Univariate and bivariate global Moran's I statistics were applied to assess the level of spatial autocorrelation in the resultant maps of the GCoS index and lower household income. The relationship between GCoS and socioeconomic indicators is driven by the association in space rather than causation. Therefore, the effect of spatial autocorrelation in the (Pearson's) correlation and vice-verse is not an issue, assuming that both metrics are capturing the association in space. The only exception is population density, which can indirectly cause low GCoS. All the correlation values showed are statisticly significance (Supplementary Information, Table 1). The

similarities among urban areas and socioeconomic indicators were visualised using heatmaps. We provide all the code used in the data processing and statistical analysis freely (see the "Code availability" section). The platform R version 4.3.1 (The R Foundation for Statistical Computing) was used for data processing, analysis and visualization. Inkscape 1.0.2 (open-source) was used to design the infographics and mosaic R plots.

Data availability

The model inputs used in this study and the resultant maps are publicly available on the original open access source (Extended Data Tab. 1). The EC measurements used to validate the model should be requested for each location separately. The social indicators are available at the ArcGIS Living Atlas of the World under the Esri agreement or at the national census bureau of each country. Esri provides the standardisation and redistribution of the indicators in granulated points from the sources: Michael Bauer Research GmbH (EU), Nexiga (DE), AIS and Instituto Nacional de Estadistica (Spain), and 4orange (The Netherlands). The green cooling simulations and the 10 m resolution GCoS maps for all functional urban areas are available at the repository 10.5281/zenodo.10708300. Functional Urban Areas (FUA) from Global Human Settlement Layer (GHSL-FUA)[67] used to define the urban areas is available at https://jeodpp.jrc.ec.europa.eu/ftp/jrc-opendata/GHSL/GHS_STAT_UCDB2015MT_GLOBE_R2019A/V1-2/ (last accessed: 04/04/2023).

Code availability

The SCOPE model (2.0) code for MATLAB (R2018b or higher) is available at[68]. The R package to download, pre-process the input data and run the SCOPE model is available by rSCOPE (2.0)[69] at https://doi.org/10.5281/zenodo.6204580. The code to calculate and map the GCoS index is available at https://github.com/AlbyDR/GCoS (https://doi.org/10.5281/zenodo.10708300).

51. Votsis, A. Planning for green infrastructure: The spatial effects of parks, forests, and fields on Helsinki's apartment prices. Ecol. Econ. 132, 279–289 (2017).
52. van der Tol, C., Verhoef, W., Timmermans, J., Verhoef, A. & Su, Z. An integrated model of soil-canopy spectral radiances, photosynthesis, fluorescence, temperature and energy balance. Biogeosciences 6, 3109–3129 (2009).
53. Yang, P., Prikaziuk, E., Verhoef, W. & Tol, C. Van Der. SCOPE 2 . 0 : A model to simulate vegetated land surface fluxes and satellite signals. 1–26 (2020) doi:https://doi.org/10.5194/gmd-2020-251.
54. European Environment Agency. Copernicus Land Monitoring Service High Resolution land cover characteristics. Imperviousness 2018, Imperviousness Change 2015 – 2018 and Built-up 2018. Online

Permalink: 7860bc42f4c1494599f1e135c832788c (2018).
55. Lang, N., Jetz, W., Schindler, K. & Wegner, J. D. A high-resolution canopy height model of the Earth. (2022).
56. Martins, J. P., Trigo, I. & Freitas, S. C. e. Copernicus Global Land Operations "Vegetation and Energy" "CGLOPS-1". Copernicus Glob. L. Oper. 1–93 (2020).
57. Hersbach, H. et al. The ERA5 global reanalysis. Q. J. R. Meteorol. Soc. 146, 1999–2049 (2020).
58. Vulova, S. et al. Remote Sensing of Environment City-wide , high-resolution mapping of evapotranspiration to guide climate-resilient planning. Remote Sens. Environ. 287, 113487 (2023).
59. Vulova, S. et al. Modeling urban evapotranspiration using remote sensing, flux footprints, and artificial intelligence. Sci. Total Environ. 786, 147293 (2021).
60. Stagakis, S., Chrysoulakis, N., Spyridakis, N., Feigenwinter, C. & Vogt, R. Eddy Covariance measurements and source partitioning of CO2 emissions in an urban environment: Application for Heraklion, Greece. Atmos. Environ. 201, 278–292 (2019).
61. Järvi, L. et al. Uncertainty of eddy covariance flux measurements over an urban area based on two towers. Atmos. Meas. Tech. 11, 5421–5438 (2018).
62. Järvi, L. et al. Seasonal and annual variation of carbon dioxide surface fluxes in Helsinki, Finland, in 2006-2010. Atmos. Chem. Phys. 12, 8475–8489 (2012).
63. Hertwig, D. et al. Urban signals in high-resolution weather and climate simulations: role of urban land-surface characterisation. Theor. Appl. Climatol. 142, 701–728 (2020).
64. Helfter, C. et al. Spatial and temporal variability of urban fluxes of methane, carbon monoxide and carbon dioxide above London, UK. Atmos. Chem. Phys. 16, 10543–10557 (2016).
65. Grimmond, C. S. B. et al. The international urban energy balance models comparison project: First results from phase 1. J. Appl. Meteorol. Climatol. 49, 1268–1292 (2010).
66. Zhou, W., Cao, W., Wu, T. & Zhang, T. The win-win interaction between integrated blue and green space on urban cooling. Sci. Total Environ. 863, 160712 (2023).
67. Florczyk, Aneta; Corbane, Christina; Schiavina, Marcello; Pesaresi, Martino; Maffenini, Luca; Melchiorri, Michele; Politis, Panagiotis; Sabo, Filip; Freire, Sergio; Ehrlich, Daniele; Kemper, Thomas; Tommasi, Pierpaolo; Airaghi, Donato; Zanchetta, Luigi (2019): GHS-UCDB R2019A - GHS Urban Centre Database 2015, multitemporal and multidimensional attributes. European Commission, Joint Research Centre (JRC) [Dataset] doi: 10.2905/53473144-b88c-44bc-b4a3-4583ed1f547e.
68. van der Tol, C. & Prikaziuk, E. SCOPE. at https://doi.org/https://doi.org/10.5281/zenodo.4309327, 2020. (2020).
69. Rocha, A. D. AlbyDR/rSCOPE: rSCOPE v1.0. at https://doi.org/10.5281/zenodo.6204580 (2022).

Acknowledgements This work was funded by the Deutsche Forschungsgemeinschaft (DFG, German Research Foundation) within the Research Training Group "Urban Water Interfaces" (GRK 2032-2), ADR. Einstein Research Unit "Climate and Water under Change" (CliWaC) from the Einstein Foundation Berlin and Berlin University Alliance (ERU-2020-609), SV. The EC data from Berlin provided by the Urban Climate Observatory (UCO) was supported by Urban Climate Under Change [UC]², funded by the German Ministry of Research and Education (FKZ 01LP1602A), FM. The EC observations in Amsterdam have been supported by the Institute for Advanced Metropolitan Solutions (AMS Institute, project VIR16002) and the Netherlands Organisation for Scientific Research (NWO) (Project 864.14.007). We acknowledge support from the 4TU-program HERITAGE (HEat Robustness In relation To AGEing cities), funded by the High Tech for a Sustainable Future (HTSF) program of 4TU, the federation of the four technical universities in The Netherlands, GJS. EC observations of Helsinki were provided by the Research Council of Finland

(project numbers: 321527, 37549 and 335201), LJ. The authors would like to thank Christian Feigenwinter for the data from Basel (CH) used in this activity CH-BaK (2019-20) and CH-BaA(2019-20). The kind permission of British Telecom (BT) is acknowledged for the London measurements. Equipment was part-funded by the Engineering and Physical Sciences Research Council (EP/G029938/1), JFB and CH. CH also acknowledges funding from the UK Natural Environment Research Council (NE/H003169/1, NE/K002279/1, NE/T001798/2). For the Vienna EC measurements, the authors acknowledge funding from the Vienna Science and Technology Fund (10.47379/ESR20030) and the City of Vienna (MA7-596744/17), as well as the support of A1 Telekom AG, BM. GN thanks the support of the ICOS Pilot Application in Urban Landscapes (PAUL) Horizon2020 Project (GA101037319). We thank three anonymous reviewers for their constructive comments on the manuscript.

Author contributions ADR, MF, SV and BK designed the overall research goals and aims. BM, CH, FM, GJS, NC, GN. GN, BG, LJ, ADR and MF were responsible for data selection and pre-processing (EC data, forcing data and socioeconomic indicators respectively). ADR conducted the data simulations, analysis and manuscript draft preparation. The manuscript received inputs about the urban areas and their climatological characteristics from BG, BK, BM, CH, FM, GJS, GN, JFB, LJ, NC, SV. All authors discussed the results and contributed to reviewing and editing the final version of the manuscript.

Competing interests The authors declare no competing interests.

Additional Information

Extended Data Tab. 1 | Model inputs and data sources used to simulate ET and soil temperature from SCOPE.

Inputs	Data sources
Leaf Area Index (LAI)	Copernicus Global Land Service [56] *http://land.copernicus.vgt.vito.be/PDF/portal/Application.html* spatial resolution: 300 m - last accessed: 30/10/2023
Canopy height (hc)	ETH Global Canopy Height 2020 [55]

	https://langnico.github.io/globalcanopyheight/ spatial resolution: 10 m - last accessed: 07/12/2022
Air temperature (Ta) Relative Humidity (RH)* Air pressure (p) Incoming shortwave radiation (Rin) Incoming longwave radiation (Rli) Wind speed (ws)	Copernicus - Climate Change Services ERA5 - ECMWF reanalysis [57] *https://cds.climate.copernicus.eu/cdsapp#!/dataset/reanalysis-era5-single-levels* *https://cds.climate.copernicus.eu/cdsapp#!/dataset/reanalysis-era5-pressure-levels?tab=overview* * spatial resolution: 0.25 degrees (lat-lon regular grid) last accessed: 10/02/2023
Sun zenith angle (tts)	Calculated based on the local timestamp.
Impervious fraction (ifr)	Copernicus – Land Monitoring Service [54] *https://land.copernicus.eu/pan-european/high-resolution-layers/imperviousness/status-maps/imperviousness-density-2018* spatial resolution: 10 m - last accessed: 03/01/2023

Extended Data Tab. 2 | Model accuracy based on hourly ET for the cities with EC tower measurements – 2019-2021

Location	**R^2**	**RMSE (mm/h)**	**relative Bias**
Amsterdam	0.41	0.034	-0.55
Basel (A/K)	0.56 / 0.62	0.032 / 0.034	-0.29 / -0.40
Berlin (TUCC/ROTH)	0.54 / **0.82**	**0.018**/ 0.025	-0.17 / **0.04**
Florence	0.21	0.020	-0.57
Helsinki	0.59	0.058	-0.21
Heraklion	0.31	0.049	-0.55
London	0.36	0.041	-0.55
Vienna	0.51	0.034	-0.25

Note: Berlin and Basel have two EC towers in the city. Values up to 24 hours after a precipitation event were excluded.

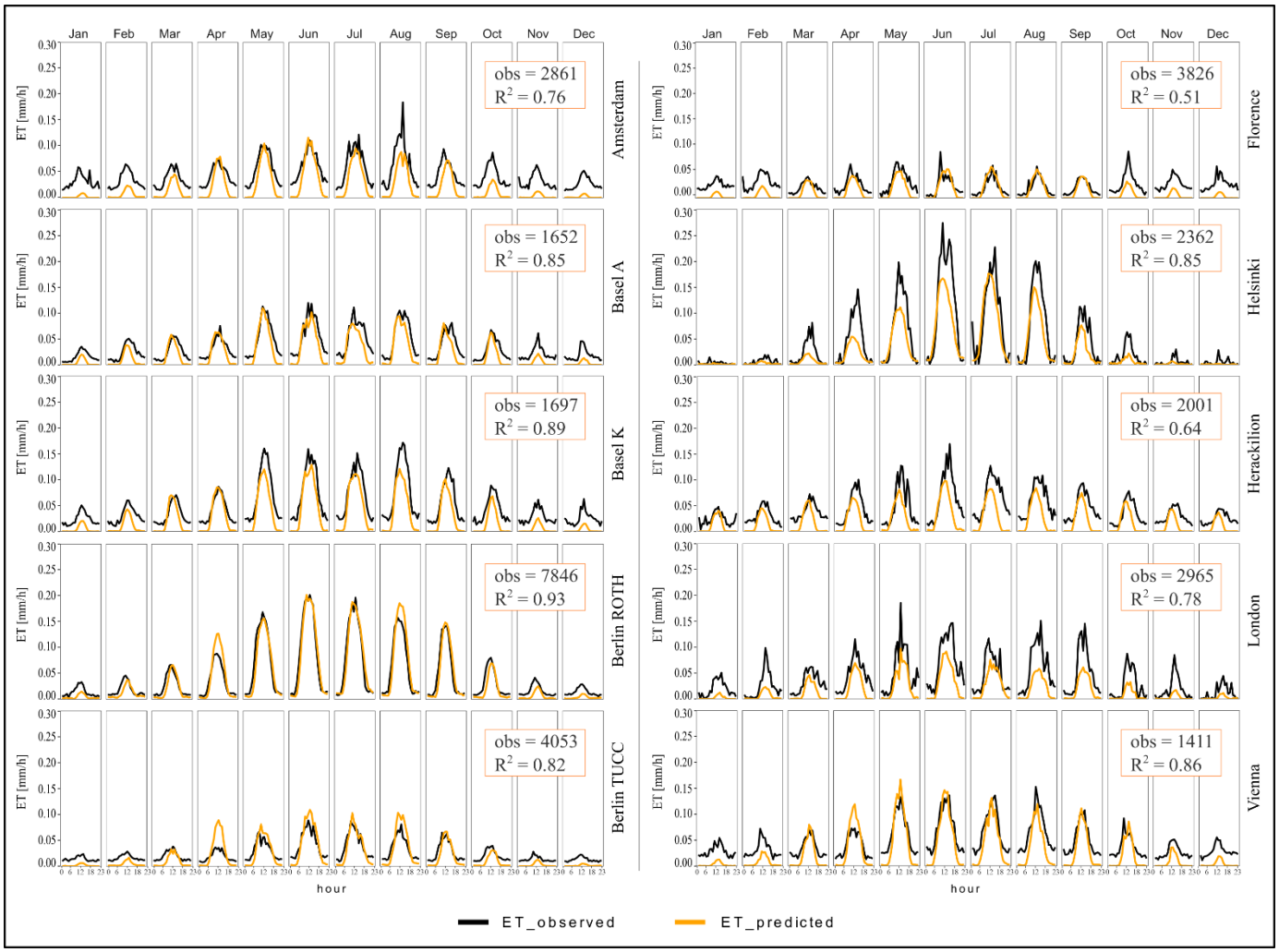

Extended Fig. 1 | Model validation of ET per month and hourly average for each urban area with EC towers measurements – 2019/2021. The values up to six hours after a rain event were excluded.

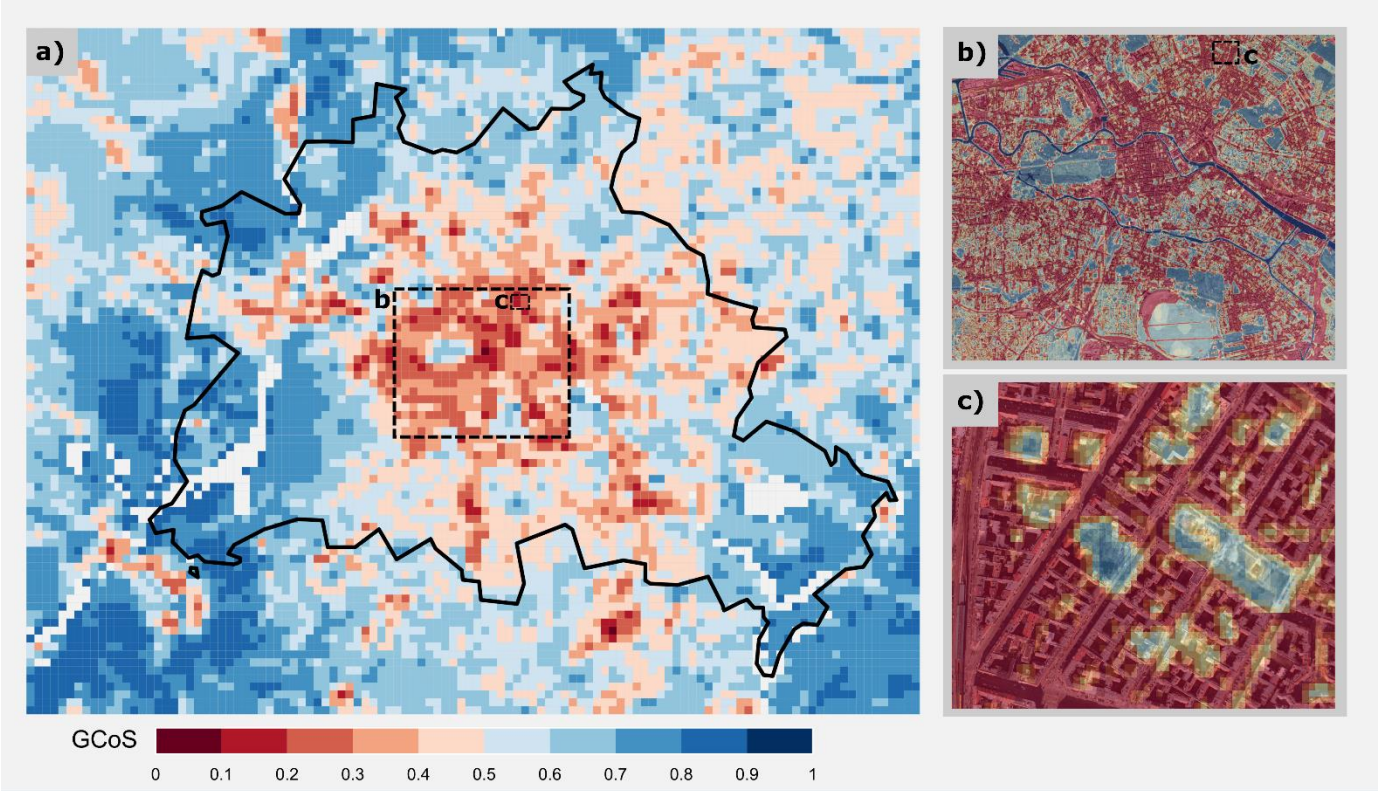

Fig. 1: Green Cooling Service (GCoS) on the hottest day in Berlin – 2012. Neighbourhood scale (a), and 10 m spatial resolution (b and c).

Extended Fig. 2 | GCoS distribution at a neighbourhood scale in Berlin (a), and at a 10 m resolution in a central area (b and c).